Multiplexed Measurements of Strain Using Short and Long Gauge Length Sensors

H Geiger, M G Xu, J P Dakin
Optical Fibre Group, University of Southampton, SO17 1BJ, UK
N C Eaton
Westland Aerospace, East Cowes, PO32 6RH, UK

ABSTRACT

The paper discusses two complimentary optical fibre sensing techniques which have been researched for structural monitoring applications. The short-gauge-length sensor system is based on fibre gratings and has achieved a strain resolution below 1 microstrain. The long-gauge-length sensor system has achieved 100 micron spatial resolution using a new OTDR technique. Results are presented for surface-mounted and embedded sensors. Both sensors systems can be multiplexed to make more efficient use of the interrogating unit. Their system designs should be capable of being developed to meet real engineering applications.

1 Introduction

Optical fibre sensors are attractive transducers for use in structural monitoring systems and for smart structure applications. In order to find eventual application in aerospace systems and in civil engineering structures, well engineered systems will be necessary. These must make use of components capable of meeting the reliability and stability requirements.

Complimentary concepts for long-gauge-length and short-gauge-length sensors are desirable to allow measurement of both major structural distortions and localised strains at selected key points. We present new results for surface-mounted and embedded sensors with two recently demonstrated interrogation systems.

2 Long-Gauge-Length Sensors Using a Precision Pseudo-Random OTDR System

Our long-gauge-length sensor consists of a novel precision OTDR system,[1] which measures the optical range of reflective markers using a guided wave LIDAR method (Fig 1). The semiconductor light source is intensity modulated using an orthogonal pseudo-random code, and the detected signal is electrically cross-correlated with a delayed version of the originally transmitted code.

2.1 Description of Method

The method relies on the fact that the correlation function arising in our receiver consists of a series of triangular peaks (Fig 2). Our method is the first to take advantage of the triangular shape of the correlation function when interrogating rectangular signals.[1] Pseudo-random encoding is used to enhance the signal-to-noise ratio (SNR) in OTDR systems.[2]

The transmitted signal is subjected to a continuously-swept electronic delay and is correlated with the detected return signals. The resulting triangular peaks, in the curve of correlation-signal versus delay, are processed by linear curve fitting to their rising and falling edges, thereby allowing precise location of the peaks from the crossover point. The method may examine the relative time delay between peaks corresponding to reflections from adjacent reflective points. A measurement of the two-way optical delay in each fibre section is, to a first order, independent of any electronic and optoelectronic delays and also of any propagation delay in the fibre interconnection lead.

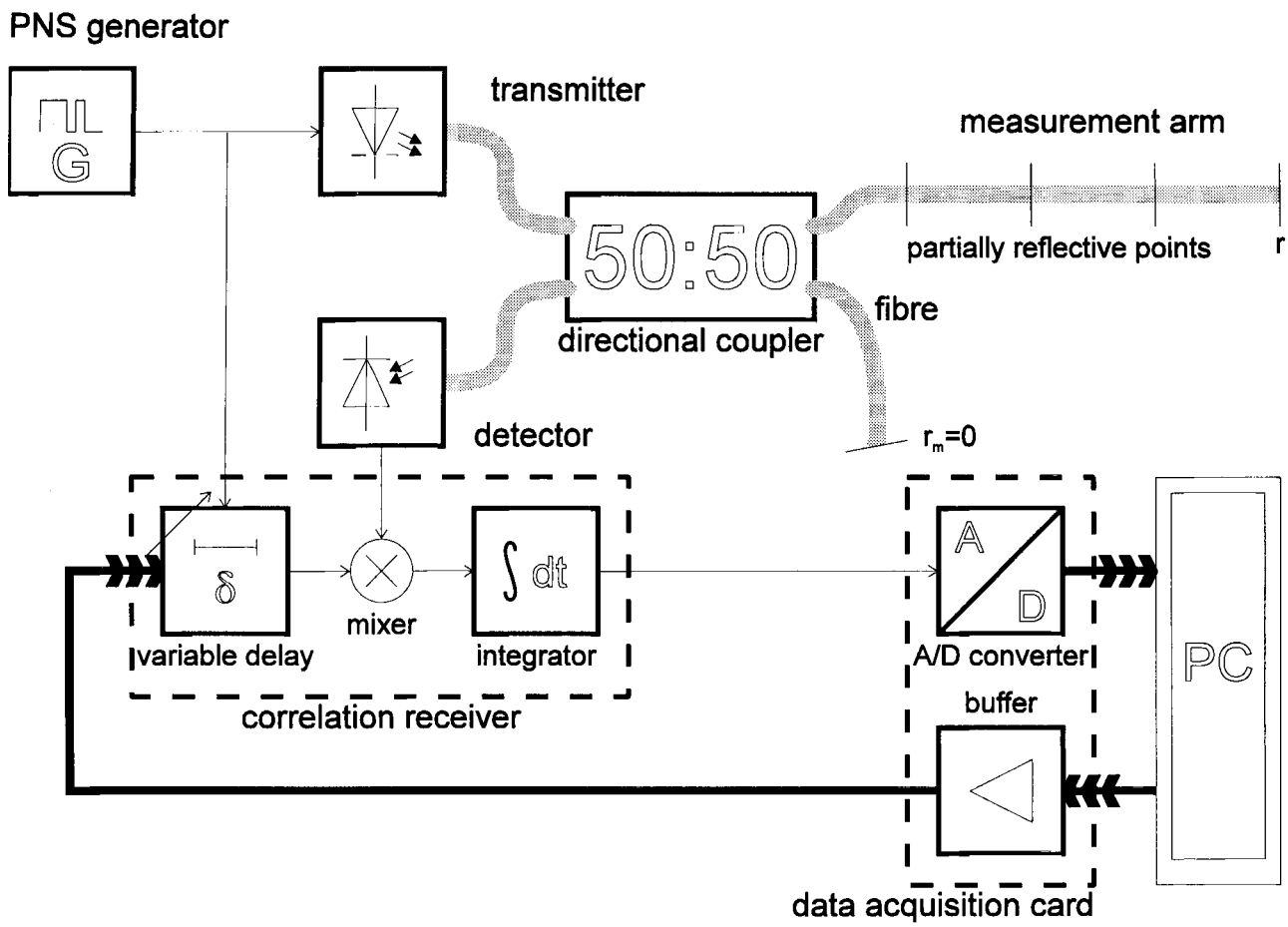

Fig 1 Enhanced OTDR

2.2 Results

Analysis of the propagation delay in an optical fibre shows that the optical path length is less affected by the applied strain than the physical length.[3] To establish that, a fibre was clamped over 1.5 m length and cleaved at the end. One clamp was mounted on a micrometer-controlled stage to allow the fibre to be stretched by a known amount (Fig 3).

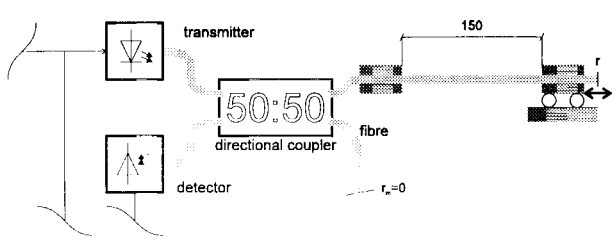

Fig 3 Calibration arrangement for unconstrained optical fibre

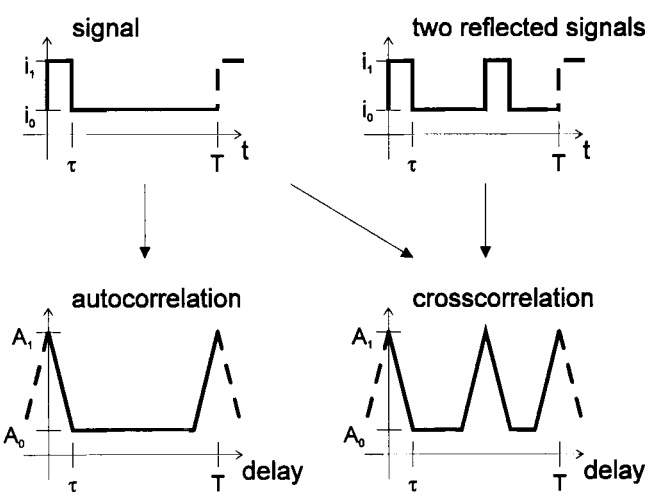

Fig 2 Correlation of a pulse of length τ with itself (*autocorrelation*) and with two similar pulses (*crosscorrelation*)

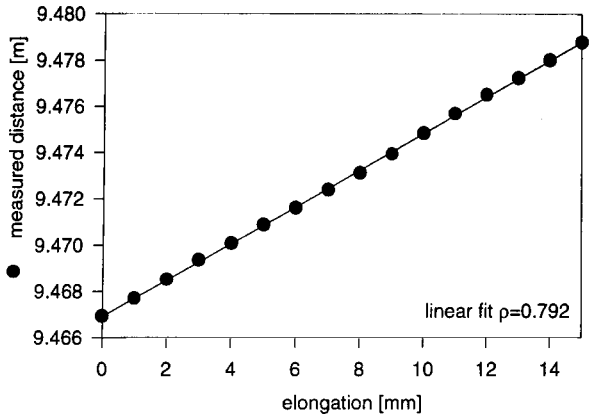

Fig 4 Measured distance as a function of fibre elongation of a unconstrained fibre

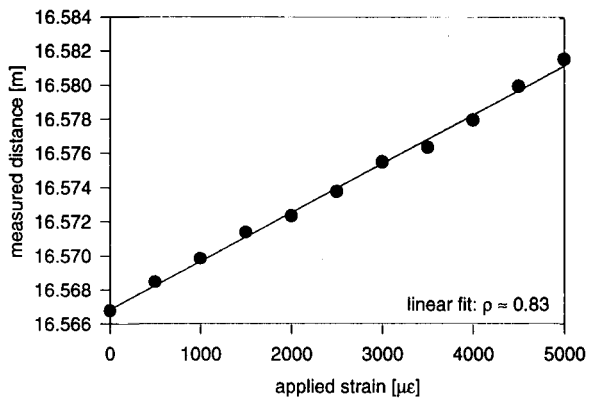

Fig 5 Measured distance of a gradually strained fibre embedded in a composite

Fig 4 displays the measured optical path length against the applied physical elongation. A linear fit to the data reveals a responsivity of 0.79 in good agreement with the theoretically predicted value.[3] This measured value is incorporated in our interrogation software to allow display of either the optical path length or a relative change of distance where a correction factor has been applied.

A similar experiment has been performed using optical fibre embedded in a carbon-fibre reinforced composite test coupon (Fig 8). Approximately 3.2 m of polyimide-coated optical fibre was embedded in the direction of the applied load. The distance measured by the interrogation system is displayed in Fig 5 as a function of the surface strain measured by a resistance strain gauge. Using the approximate length of the strained fibre section and assuming a uniform strain field, a responsivity of 0.83 is derived.

2.3 Real-Time Measurements

Our OTDR interrogation system initially scans the fibre response over a selected region and displays it. The software finds peaks and identifies the slopes of the peaks (cf Fig 2). To improve the SNR, further scans acquire only data from the slopes of the peaks (Fig 6, top right). The delay computed for each scan is subsequently plotted as a function of elapsed time (Fig 6, bottom left). The step response seen is the response to a 1.5 mm elongation of the interrogated fibre without compensation of the fibre responsivity. The software allows compensating for the responsivity and increasing the SNR by applying a digital lowpass filter.

The noise level in our latest experimental measurements corresponds to a noise-limited resolution of 100 μm RMS at a response time of 0.5 s, equivalent to a resolution of 20 με (microstrain) over a 5 m measurement section. The corresponding delay resolution of 1 ps is many orders of magnitude less than the bit period of the pseudo-random code (≈10 ns). Our most recent results are approximately 4 times better than reported in our earlier paper.[1] The main improvement arises from the use of a higher power (1 mW) source, which has improved the optical SNR.

Pseudo-random encoding enhances the SNR compared to the single pulse used in conventional OTDR, yet still permits the system to distinguish between reflections from different points. Because of the use of intensity detection, polarisation effects in the fibre should not effect the measurement and the system is relatively immune to lateral strain in the fibre. The system has the further advantage of using communications components, so should be capable of development for use in avionics systems.

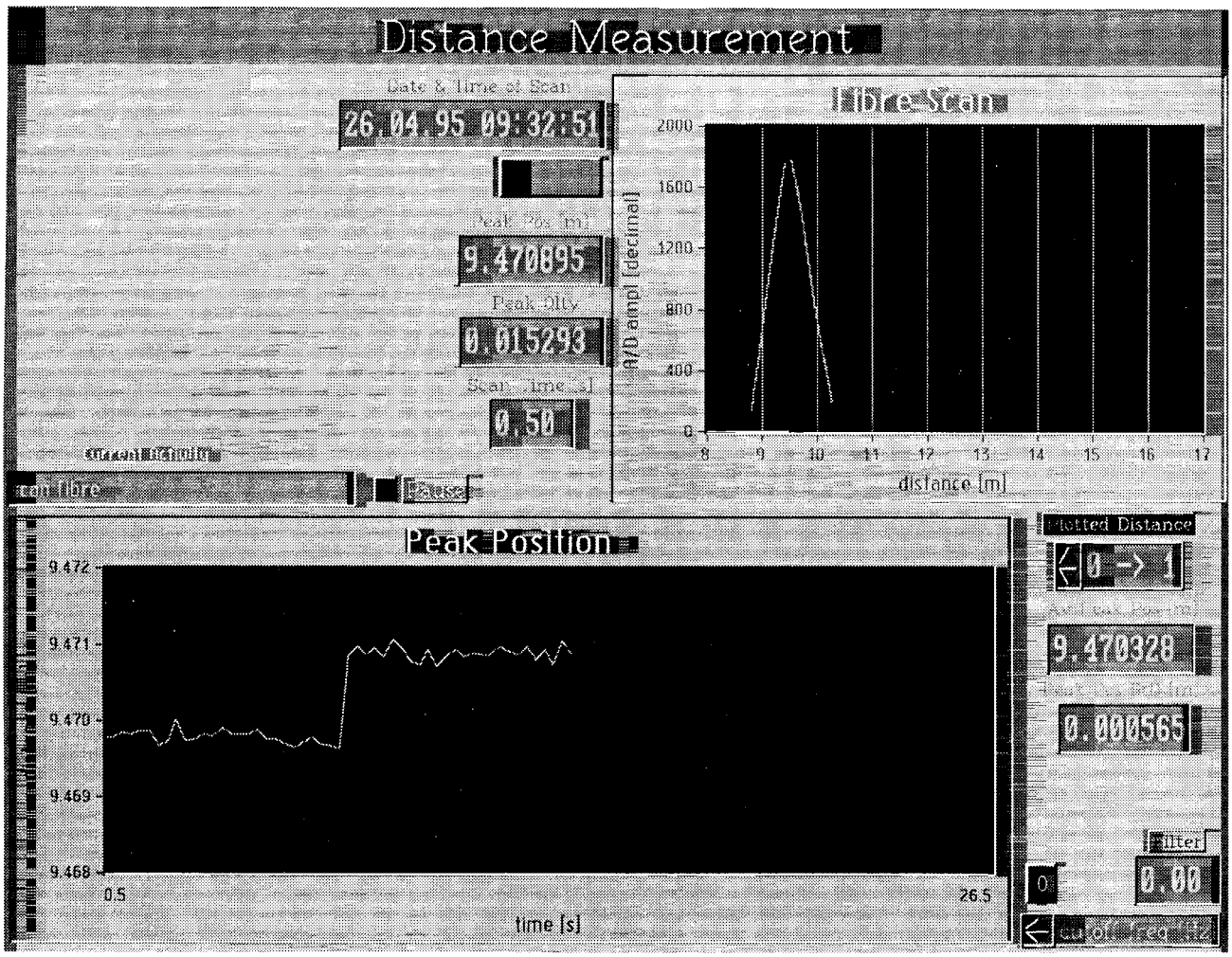

Fig 6 PC display showing the result of multiple scans plotted as a function of time

3 Short-Gauge-Length System Using An Acousto-Optic Tunable Filter

The objective of this part of our work is to develop a multiplexed system of short-gauge-length sensors by measuring the wavelength of fibre Bragg gratings. As before, the aim is to use communications components where possible.

3.1 Description of Method

Our interrogating system for fibre Bragg grating sensors uses an acousto-optic tunable filter (AOTF).[4,5] This type of optical bandpass filter may rapidly access any wavelength (tuning time ~10 s) and has a wide tuning range (about 1 octave). At constant temperature, its peak transmission wavelength is determined solely by the frequency of an RF drive signal. It is therefore suitable both for dynamic and quasi-static strain sensing and for use in multiplexed sensing systems.

Our experimental system is shown schematically in Fig 7. A broadband optical source (1300 nm ELED) illuminates the fibre gratings to be measured. The reflected light passes through the AOTF ($\Delta\lambda$ = 3.3 nm) to a detector. As already mentioned, the wavelength of the light transmitted by the AOTF is a function of the AOTF drive frequency. Thus by sweeping the AOTF, the Bragg wavelengths of a set of gratings in a fibre network can be determined.

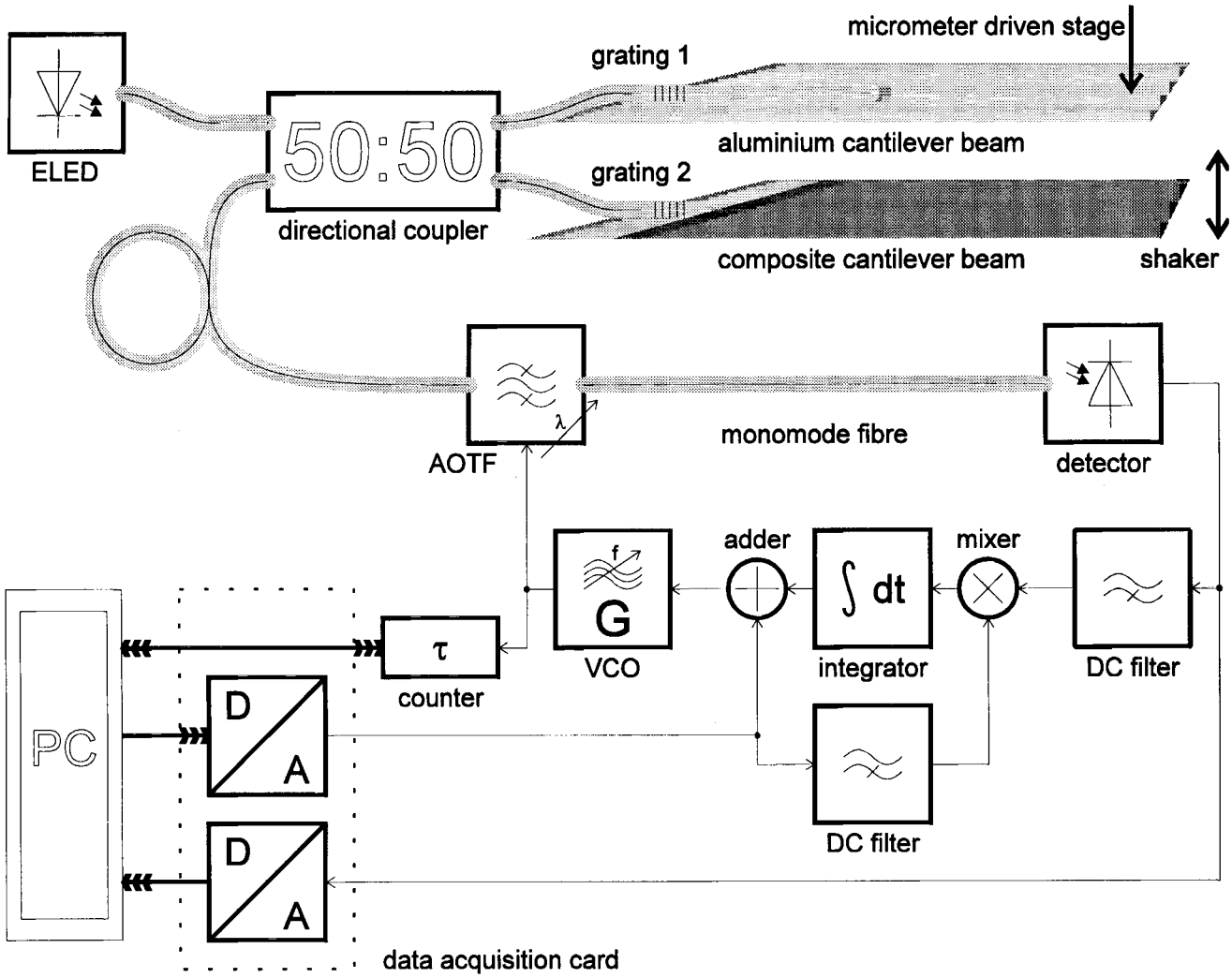

Fig 7 Block diagram of realised grating interrogation system and experimental arrangement

This sweep is carried out by computer control of an RF voltage-controlled oscillator (VCO) and the spectrum of a set of gratings can be displayed (Fig 13, upper left). An identification number is then allocated to each grating and the peak wavelength of each is stored. The computer can then instruct the system to lock onto a selected grating using the hardware loop shown in Fig 7. At this stage, the computer also displays an expanded-scale spectrum of the selected grating (Fig 13, upper right). All spectra are broadened due to interrogation by an AOTF having a greater bandwidth than the gratings.

To track the instantaneous Bragg wavelength, it is feasible to employ a feedback signal to lock the mean optical wavelength of the filter to the instantaneous Bragg wavelength of the fibre grating. This involves dithering the RF frequency applied to the AOTF about a nominal value (ie FSK modulation) and detecting the amplitude modulation (AM) of the received optical carrier. An AM signal results when the optical transmissions are different at the two extremes of the AOTF frequency excursions. Assuming that the mean AOTF wavelength is proportional to the applied RF frequency over the strain-induced wavelength shift of each fibre grating and that grating and filter responses are symmetrical, the AM signal is zero when the mean wavelength of the AOTF coincides with the Bragg wavelength of the grating. This condition can be achieved by adjusting the mean frequency of the FSK signal. The same detection system can be used to measure the Bragg wavelengths of gratings in either reflective or transmissive configurations.

3.2 Mechanical Test Arrangements

The interrogation system was tested in two different mechanical arrangements: cantilever beams and a tensile test fixture. Tests with both mechanical arrangements complement each other. A cantilever beam is convenient for the application of low levels of static and dynamic strain, but the applied strain depends on the location of the sensor on the cantilever. In contrast, a tensile test fixture allows application of higher levels of static strain, while the applied strain is essentially independent from the location of the sensor.

Although both test arrangements allow a computation of the strain from the applied force or from the applied deflection, a direct measurement of the surface strain was made with a resistance strain gauge.[6]

3.2.1 Cantilever Beams

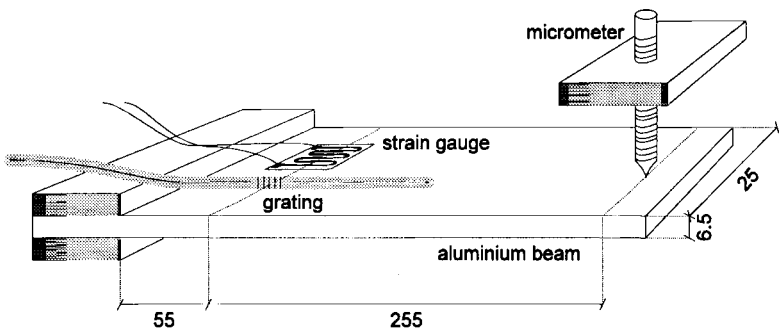

Fig 9 Aluminium cantilever beam

Two separate cantilevered beams were used to test both surface-mounted and embedded gratings. One grating was surface-mounted on an aluminium beam, at the same distance from the fixed end as a conventional strain gauge to experience the same strain (Fig 9). A micrometer-driven stage allowed a fine control of the vertical beam deflection. This beam was used to calibrate the systems strain response.

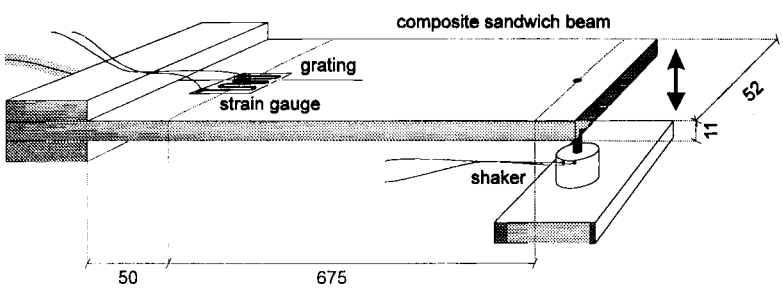

Fig 10 Composite cantilever beam

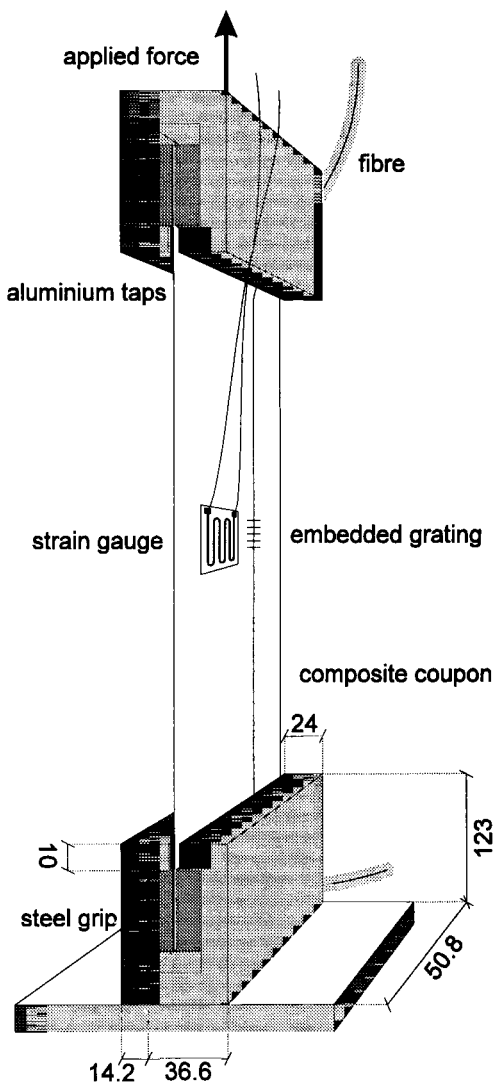

Fig 8 Tensile test fixture; the strain gauge is actually placed on top of grating.

The second cantilever beam is a composite sandwich structure. Carbon-fibre reinforced composite material encloses a honeycomb material, resembling a typical aerospace structure (Fig 10). The grating was embedded in the top composite sheet between the lower two of three plies, approximately 0.25 mm below the surface. The composite fibres were aligned in the direction in parallel with the optical fibre. A strain gauge was surface-mounted above the grating. The beam tip was deflected by an electrodynamic shaker driven by an audio signal generator.

3.2.2 Tensile Tests

Test samples of composite materials were clamped in a tensile test fixture to strain both composite and optical fibre (Fig 8). Three test samples with embedded fibre were strained until mechanical failure. The composite always failed before the embedded fibre, encouraging the use of optical fibre as a sensing medium.

3.3 Static Measurements

The system was calibrated by mounting gratings next to resistance strain gauges and applying static loads. The mean AOTF frequency was read and plotted against the strain measurements using a commercial resistance strain gauge amplifier.

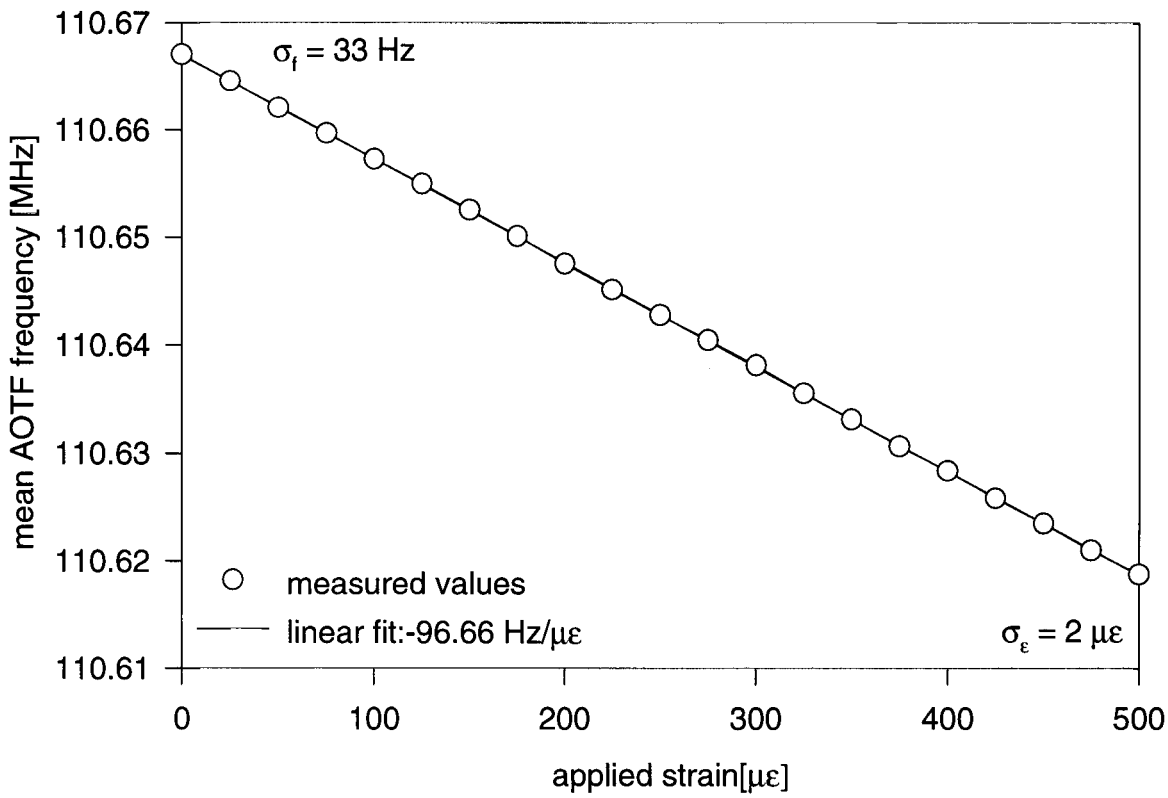

Fig 11 Calibration of AOTF frequency against applied strain: linear fit and standard deviations of strain and frequency measurement

The change of the mean AOTF frequency due to applied strain was recorded using the aluminium cantilevered beam (Fig 9). The system tracked the grating, and a scale factor of -96.7 Hz/με was determined by recording the mean AOTF frequency (Fig 11).

Additionally, a similar experiment was performed using the tensile test fixture (Fig 8). The embedded fibre had two gratings with 0.2 and 0.35 nm bandwidth whose Bragg wavelengths were just 0.95 nm apart. Since the bandwidth of the AOTF was 3.3 nm, only one peak was detected by the interrogation system. The composite sample was strained until it broke just under 4300 με and the AOTF output is shown in Fig 12. For comparison, the grating peaks were also monitored with a laboratory spectrum analyser and these results are shown as well.

In common with many other optical filters, AOTFs are temperature sensitive. Tracking an unstrained grating held at constant temperature while slowly changing the AOTF temperature, a variation of the mean AOTF frequency of 2.68 kHz/K is

measured; ie a 1 K increase in the AOTF temperature results in a signal equivalent to a (compressive) strain of -27.7 με.

3.4 Real-Time Measurements

After scanning the spectrum of the optical subsystem, the PC displays the recorded data (Fig 13, top left). The user selects a grating and starts the lock-in mode. An initial fine scan of the chosen grating identifies the points on the slope of the spectrum that will result in the highest sensitivity to wavelength changes (Fig 13, top right). The system uses the wavelength difference between these points to set the frequency deviation of the FSK in the lock-in mode.

The counter measures the mean AOTF frequency over a measurement period set by the user (Fig 13, bottom right). The measured frequency is displayed (Fig 13, middle right) and the frequency change against time may be plotted in real-time. In Fig 13 the mean AOTF frequency is plotted as its equivalent strain (Fig 13, bottom left).

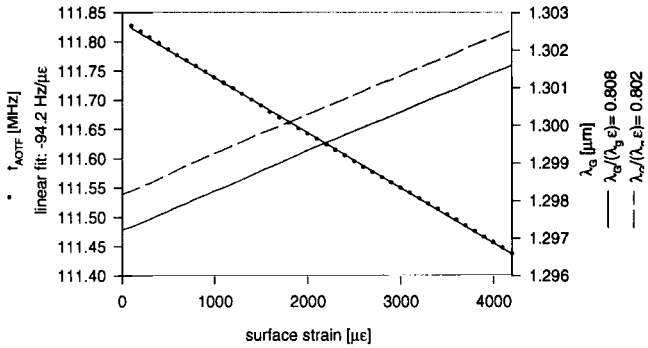

Fig 12 AOTF frequency and Bragg wavelength of two embedded gratings which are too close together to be distinguished

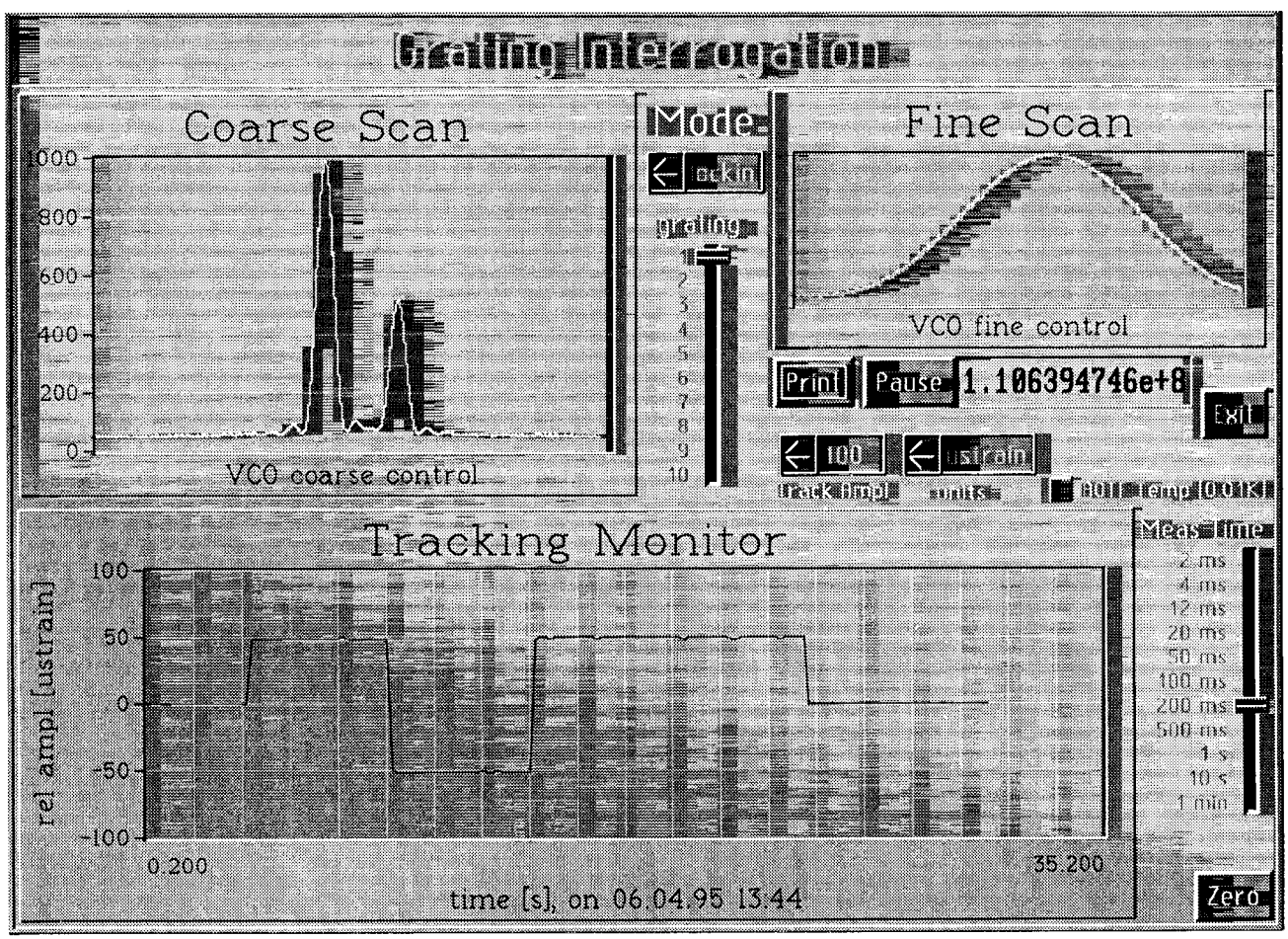

Fig 13 PC display showing applied quasi-static strain (grating 1, measurement period per point: 100 ms)

The measurement was obtained while tracking grating 1 (cf Fig 7) which was surface-mounted on an aluminium cantilever beam (Fig 9). Strain was applied by deflecting the beam with a micrometer-driven stage. After an initial measurement with no strain, a strain cycle of 50 με, -50 με, and 50 με was applied before returning to the initial condition. With a measurement period of 100 ms, the trace shows negligible noise beyond the quantisation noise caused by the limited resolution of the PC display.

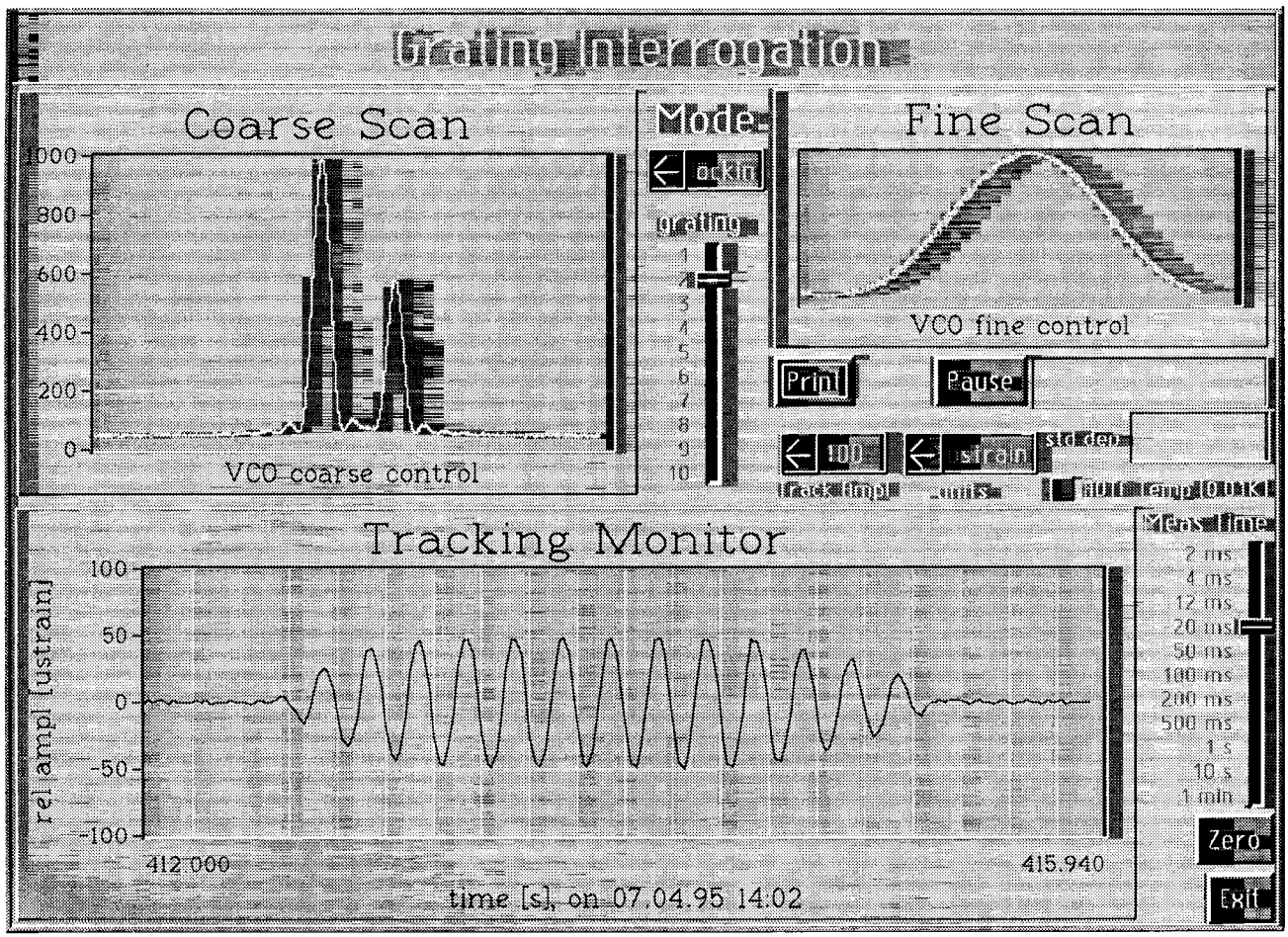

Fig 14 PC display showing applied dynamic strain (grating 2, measurement period per point: 20 ms)

Tracking dynamic signals is also possible. Fig 14 shows the response of grating 2 embedded in a composite cantilever beam (Fig 10) and excited by a shaker. The 5 Hz excitation was gradually started and stopped. With a measurement period of 20 ms in this trace, it can be seen that the system noise is again similar to the quantisation noise level resulting from the display. Within the measurement accuracy of ± 2 με, identical values for the peak strain were measured with a conventional strain gauge mounted on the surface above the embedded grating. Fig 15 shows the excitation voltage at the shaker (top trace) and the output voltage from the commercial resistance strain gauge amplifier.

4 Conclusions

We have successfully developed a long-gauge-length and short-gauge-length sensing system for strain monitoring. Each approach uses a simple optical arrangement and sophisticated signal processing, and should be adaptable for use in moderately hostile environments. Both short-gauge-length sensor and long-gauge-length sensors have been tested, showing resolutions

below 1 με and 100 μm, respectively. The application of these sensors embedded in composite materials was also demonstrated.

5 Acknowledgements

The authors gratefully acknowledge Westland Aerospace, the U.K. Department of Trade and Industry, and the Engineering and Physical Science Research Council (ESPRC) for supporting this research over the last 3 years; the European Space Agency for funding the initial work on the grating interrogation system; and L. Reekie, J. Tucknott, and L. Dong for supplying the gratings.

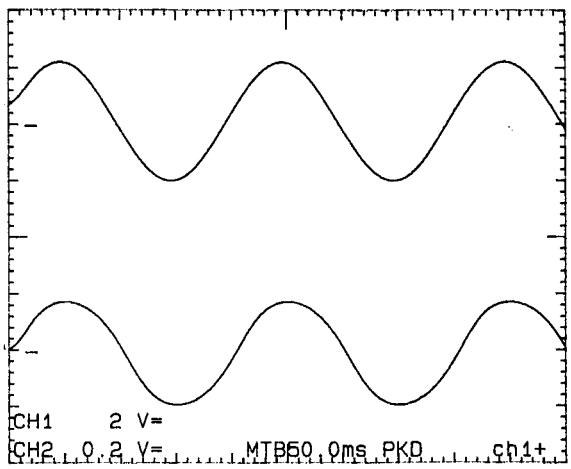

Fig 15 5 Hz excitation (top) and bridge voltage from a strain gauge amplifier (bottom), both filtered at 17 Hz

6 References

1. Geiger H, Dakin J P, "Low-cost high-resolution time-domain reflectometry for monitoring the range of reflective points", to appear in *Journal of Lightwave Technology*, July 1995

2. Okada K, Hashimoto K, Shibata T, Nagaki Y, "Optical cable fault location using correlation technique", *Electronics Letters*, vol 16, no 16, 1980

3. Hocker G B, "Fiber-optic sensing of pressure and temperature", *Applied Optics*, vol 18, no 9, pp 1445-1448, 1979

4. Xu M G, Geiger H, Archambault J-L, Reekie L, Dakin J P, "Novel interrogating system for fibre Bragg grating sensors using an acousto-optic tunable filter", *Electronics Letters*, vol 29, no 17, pp 1510-1511, 1993

5. Geiger H, Xu M G, Eaton N C, Dakin J P, "Electronic tracking system for multiplexed fibre grating sensors", *Electronics Letters*, vol 31, no 13, 1995

6. People J, "BSSM Strain Measurement Reference Book", *British Society for Strain Measurement*, ISBN 0-9506351-0-3, 1979